Available online at www.sciencedirect.com

ScienceDirect

Procedia Structural Integrity 2 (2016) 2381–2388

Structural Integrity Procedia

www.elsevier.com/locate/procedia

21st European Conference on Fracture, ECF21, 20-24 June 2016, Catania, Italy

Microstructure and directional fatigue behavior of Inconel 718 produced by selective laser melting

Radomila Konečná[a], Gianni Nicoletto[b], Ludvík Kunz[c], Adrián Bača[a],

[a]*University of Žilina, Dept. of Materials Engineering, Žilina, Slovakia*
[b]*University of Parma, Dept. of Industrial Engineering, Parma, Italy*
[c]*Institute of Physiscs of Materials, Brno, Czech Republic*

Abstract

Recent research efforts in additive manufacturing have focused on developing parts made of Inconel 718 (IN 718), a nickel-based superalloy, which is an attractive material for aerospace and energy high-temperature applications. Here the selective laser melting (SLM) process is used to transform alloy powder into a solid IN 718 parts followed by optimal stress-relief and subsequent precipitation hardening treatment. Two main aspects were investigated. The IN 718 microstructure generated by the SLM process was characterized using metallographic techniques and found to be distinctly directional because it is a result of a layer-by-layer material build-up typical of the SLM process. The high cycle fatigue behavior of SLM IN 718 was determined using a novel test method designed to determine and quantify the directional material behavior, which is important information for part design and process optimization. The fatigue S-N data show that the direction parallel to the build direction is associated with the lowest fatigue strength. The role of the as-produced surface characteristics on fatigue crack initiation is discussed.

Peer-review under responsibility of the Scientific Committee of ECF21.

Keywords: Selective laser melting; Inconel 718; microstructure; fatigue; crack initiation.

1. Introduction

There are a number of different technologies used in the metal Additive Manufacturing systems available today. Selective laser melting is an additive manufacturing process that uses 3D CAD data as a digital information source

* Corresponding author. Tel.: +421 41 513 2604;
E-mail address: radomila.konecna@fstroj.uniza.sk

Peer review under responsibility of the Scientific Committee of ECF21.
10.1016/j.prostr.2016.06.298

of the part geometry and a high-power laser beam as a focused heat source to create three-dimensional metal parts by layer-by-layer melting of fine metal powder, Gibson et al. (2014).

Recent research efforts have focused on developing parts made of IN 718, a nickel-based superalloy, which is an attractive material for aerospace and high-temperature applications in power generation, Wang et al. (2012).

The SLM process is characterized by high localized thermal gradients and rapid solidification. The result is a complex microstructure and residual stress build up, Kruth at al. (2007) and Mercelis et al. (2006). A previous study by Konečná et al. 2016 indicated that residual stresses produced by the SLM process may have an influence on the fatigue crack growth measured in SLM IN 718 compact-tension (CT) specimens. Interaction of residual stresses in as produced specimens with the propagating fatigue crack resulted in low crack propagation threshold, $\Delta K_{th,}$ because the crack remained always open during the entire load cycle.

The investigation presented here had two main aims: 1) the characterization of the IN 718 microstructure generated by the SLM process using metallographic techniques; 2) determination of the high cycle fatigue strength of SLM IN 718 after an optimal stress-relief treatment followed by a double precipitation hardening treatment.

2. Experimental details

2.1. The selective laser melting process

Powder-bed based additive manufacturing systems typically use a powder deposition method consisting of a coating mechanism to spread a powder layer onto a substrate plate and a powder reservoir, see Fig. 1. Once the powder layer is distributed, a laser beam applied to the powder-bed melts a 2D slice under inert gas atmosphere (in vacuum). The melting process is repeated layer after layer, until the part is complete. Then the part is removed from the powder-bed and post processed according to requirements. Here a RENISHAW 250 system (Renishaw, UK) implemented the SLM process and optimized process parameters. The 200 W Ytterbium fiber laser produced layers 30 µm in thickness.

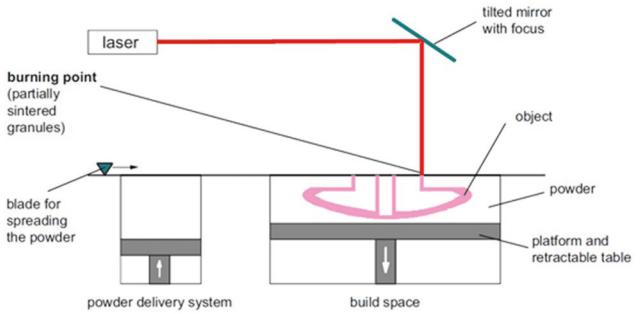

Fig. 1. Scheme of the Selective Laser Melting powder-bed process (VDI 3404).

2.2. SLM IN 718

The SLM system processed a pre-alloyed IN 718 alloy in fine powder form with globular particles 24 - 53 µm diameter range. The chemical composition of the experimental material, determined by spectrometry, is given in Tab. 1.

Table 1. Chemical composition of IN 718 powder.

Element	Ni	Cr	Fe	Nb	Mo	Co	Ti	Al	Cu
Wt. %	51.56	17.9	18.2	5.23	3.21	0.15	1.14	2.19	0.05

After the SLM fabrication phase, the following optimized heat treatment cycle was applied: i) stress relief (heating to 970 °C for 1 hour followed by cooling in Argon atmosphere) ii) age hardening (heating to 710 °C for 8 hours, further aged at 610 °C for 8 hours and final cooling to room temperature in Argon).

The Rockwell C hardness of SLM IN 718 after hardening was determined using a digital Rockwell RR-1D/AC hardness tester. Ten HRC measurements were converted to Vickers hardness and an average value of 449 HV was obtained. In the previous study by Konečná et al. 2016, it was found that the Vickers hardness of the SLM IN 718 in as-fabricated state was 338 HV. The present hardening treatment therefore resulted in a 100 HV hardness increase. Tensile tests on specimens with machined surfaces provided the following reference properties for the material, process and heat treatment: ultimate stress R_m= 1406 MPa, yield stress $R_{p0.2}$ = 1213 MPa, elongation to rupture A = 19 %.

Metallographic specimens cut from samples were prepared according to standard techniques and then observed using the Neophot 32 light microscope and Tescan LYRA 3 XMU FEG/SEM with EDX analysis system. Microstructure was analyzed after etching with Kalling's reagent (2 g of $CuCl_2$, 40 ml of HCl, 80 ml of methanol) and etching agent with composition HCl + H_2O_2 (especially for SEM analysis).

2.3. Fatigue test method

A new fatigue testing methodology based on a miniature specimen geometry developed and presented by Nicoletto (2016) was applied to the present SLM IN 718 with aim of determining the influence of the anisotropic microstructure due to the material fabrication process on the high cycle fatigue strength. Therefore, three sets of miniature specimens with three different orientations with respect to build, denoted as A, B and C in Fig. 2, were conveniently fabricated and heat treated. Specimen surfaces were kept in the as-fabricated state. Fatigue testing was performed in plane bending under a stress ratio R = 0 at 20 Hz loading frequency at room temperature. Tests were interrupted (i.e. run out) when specimens reached 2 x 10^6 cycles without failure.

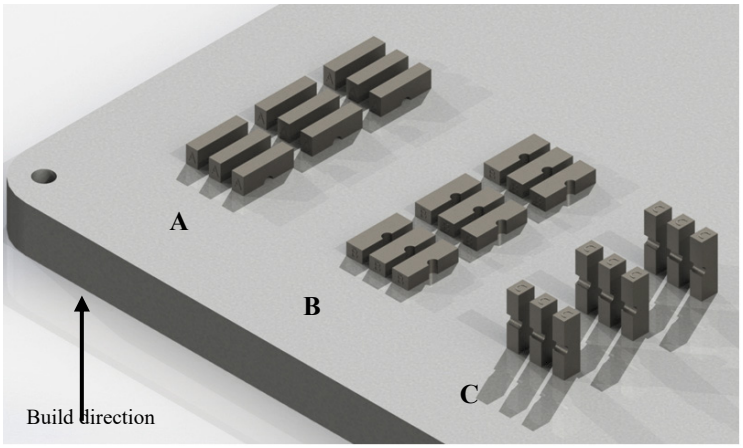

Fig. 2. Rendering of specimens layup in the build.

3. Results and discussion

3.1. Microstructure

The microstructure of SLM IN 718 is distinctly directional because it is the result of a layer-by-layer material build-up typical of the SLM process. In this case the characteristic dendritic microstructure in as-fabricated material was modified due to the heat treatment consisting in reheating (stress relief at temperature lower than that solution treatment) and double aging during which numerous precipitates form.

The characteristic microstructure after heat treatment on three perpendicular planes at high magnification is shown in Fig. 3a. The arrow indicates the SLM building direction, which coincides with the z-axis of the associated coordinate system. The microstructure revealed on x-z and y-z planes has similar features with elongated grains. It differs from that on x-y cut plane, which is perpendicular to the build direction. The microstructure revealed on the

x-y section shows equiaxed grains with slightly different size corresponding to the perpendicular sections of elongated grains. Elongated grains with variable thickness are revealed at lower magnification when etching agent (HCl + H_2O_2) is applied, Fig. 3b. Fig. 3c shows the cellular morphology of solid solution γ (face centered cubic lattice) matrix in elongated grains and numerous small carbides, which could be easily distinguished for their typical rectangular shape and their natural orange color when observed in the optical microscope.

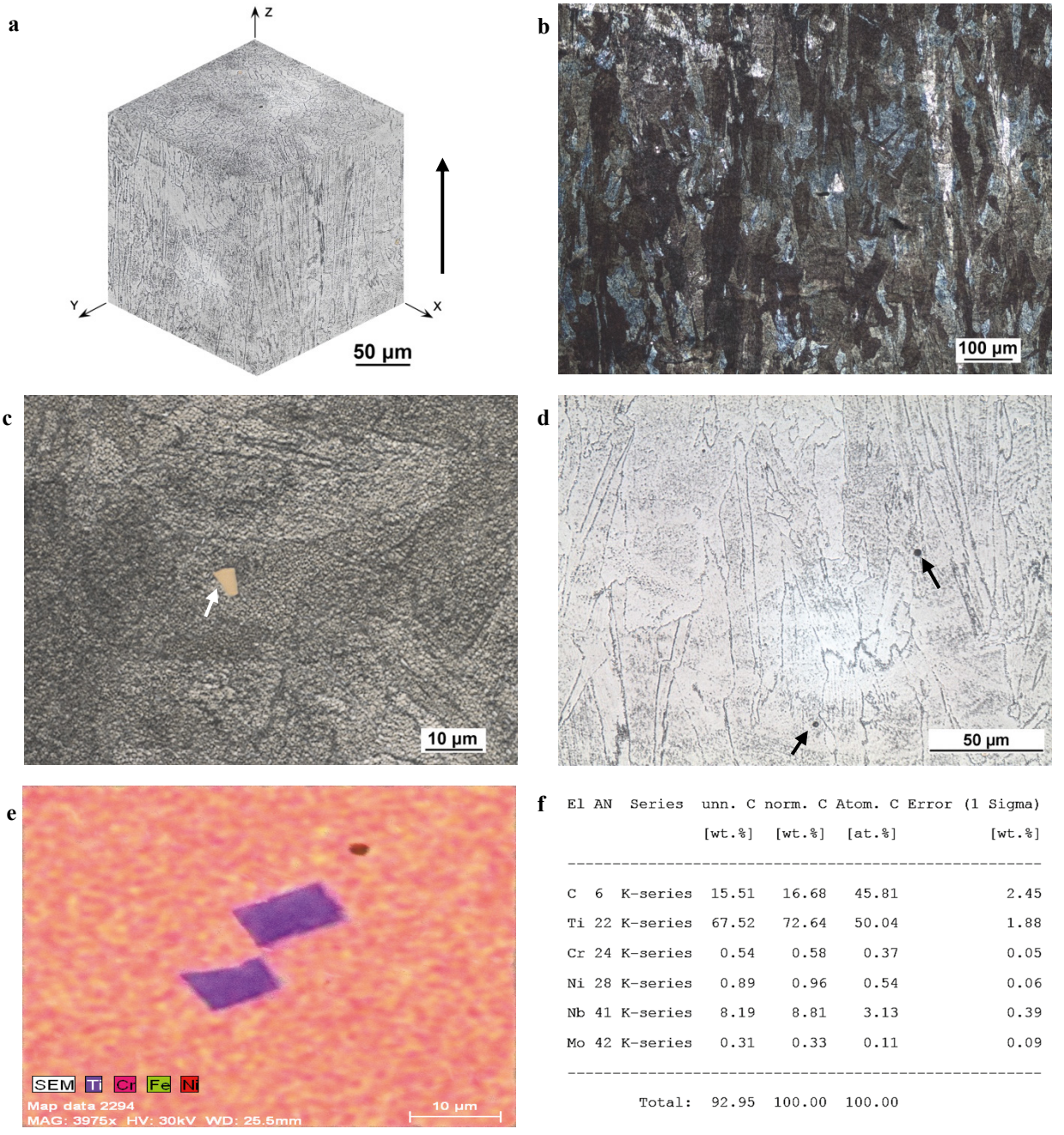

Fig. 3. Microstructure characterization of IN 718 after heat treatment, (a) 3-D microstructure etched Kalings, (b) elongated grains in the build direction, etched HCl + H_2O_2, (c) (Ti,Nb)C carbide on metallographic section (white arrow), globular shape of γ matrix, etched HCl + H_2O_2, (d) precipitates on the grain boundaries and also inside grains, black circles are gas pores (arrows), etched Kallings (e) carbides on the base Ti/Nb, etched Kallings (f) spectrum of carbides, SEM EDX analysis.

The EDX analysis confirmed that these carbides are of the MC-type. They are characterized by high content of Ti and lower content of Nb, i.e. (Ti,Nb)C type, see D. Clark et al. (2008) and G. D. Janaki Ram et al. (2005), Fig. 3e and 3f. Numerous precipitates were localized along grain boundaries and inside grains with presence of gas pores, see Fig. 3d. The composition of precipitates was determined with EDX (example Spectrum 5 in Fig. 4a). The analysis indicates high content of two elements, namely Ni and Nb, Fig. 4b. Nb-rich precipitates are considered to be Laves phases, see G. Knorovsky et al. (1989). The composition of γ matrix (spectrum 8 in Fig. 4.b) is rich in Ni, Cr and Fe, Fig. 4c.

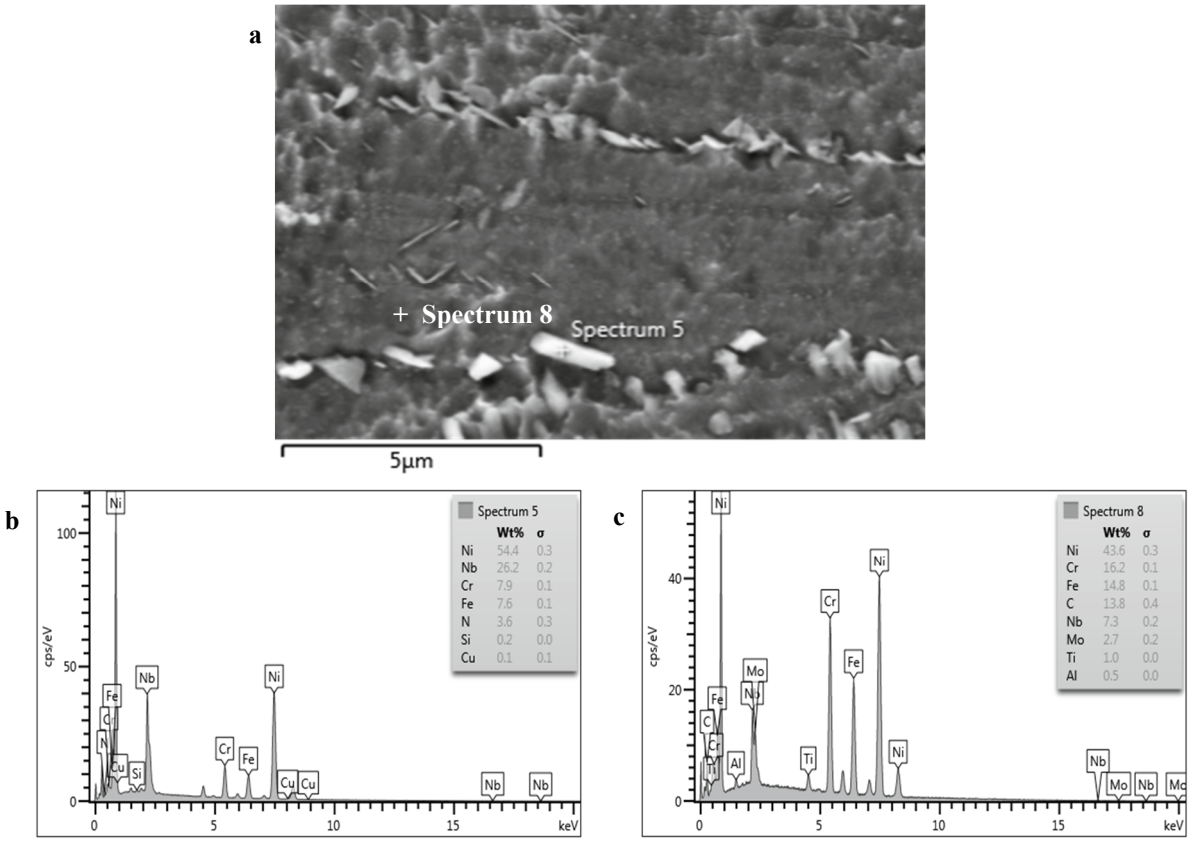

Fig. 4. SEM micrograph of precipitates in IN 718, etched HCl + H_2O_2 (a), precipitate spectrum (b) and matrix spectrum (c).

During double aging, γ′ (intermetallic compound with stoichiometric composition $Ni_3(Al, Ti)$ characterized by face centered cubic lattice) and γ″ (stoichiometric composition Ni_3Nb) phases disperse and precipitate into the matrix to strengthen the alloy, Z. Wang et al. (2012). High similarity of both γ and γ′ lattices leads to a prolonged coherent hardening.

3.2. Directional fatigue behavior

Inspection of the material microstructure shown in Fig. 3 along with the specimen orientation with respect to build shown in Fig. 2 clarifies the direction of the applied bending stress with respect to the layer-by-layer material structure. Namely, stress direction in C specimens is orthogonal to the material layers, the stress in A specimens in the plane of the last solidified layer, while the stress direction in B specimens is parallel to the layers.

High-cycle fatigue test data for the three specimen orientations are shown in Fig. 5. First, the scatter in the data for the same configuration is rather low suggesting that the material structure variability within the specimen cross-

section (i.e. 5 x 5 mm^2) is small. The trend in a linear-log plot is well behaved with fatigue lives of the specimens with the C orientation that are considerably different and shorter than the other two specimen orientations (i.e. A and B of Fig. 2). The presence of an anisotropic fatigue behavior of SLM IN 718 is therefore demonstrated and quantified. The other two orientations show a similar behavior with a slight higher performance of orientation A. The present directional fatigue data agree with previous findings obtained with the same test method in DMLS Ti-6Al-4V by Nicoletto et al. (2015).

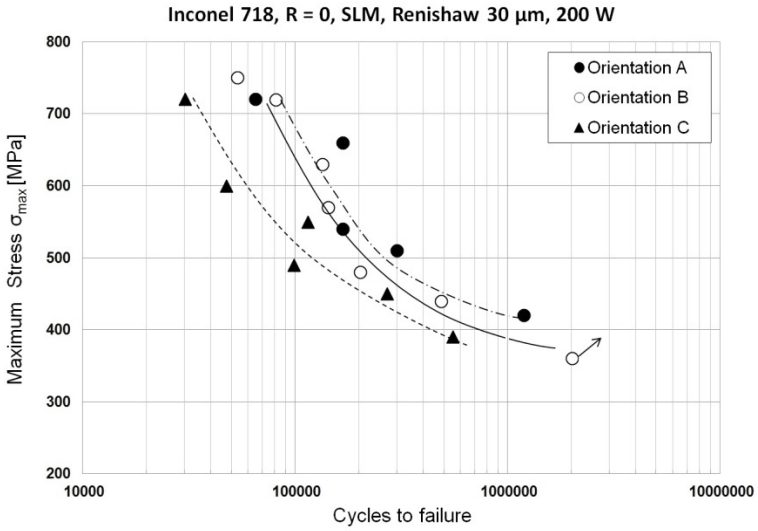

Fig. 5. Fatigue life of SLM IN 718 specimens in dependence on their orientation with respect to build orientation (see Fig. 2).

Residual stresses that develop during the SLM process can seriously influence the fatigue properties, both in terms of crack initiation and crack propagation. The present specimens were heat treated to remove the residual stress fields. The X-ray measurement of residual stresses on the specimen surfaces where the fatigue cracks initiated was performed to ensure that the stress relieving procedure was successful. Stresses in two directions were measured, namely in the longitudinal direction coinciding with the longer axis of the specimen and in the transversal direction. The measurement led to the conclusion that only very weak (i.e. not exceeding 40 MPa) compressive residual stresses are present in the surface layer.

3.3. Fatigue crack initiation from as-produced surfaces

Fig. 6 allows the discussion of two correlated aspects occurring in the case of high cycle fatigue testing: surface quality (i.e. surface roughness) and fatigue crack initiation mechanisms. Figs. 6a, 6c and 6e show the outline in white of the broken specimens, one for each orientation (fracture surface on the right) and identification of the top surface where the roughness measurement was performed (on the left). Tab. 2 provides the roughness data that show that the specimen orientation A is characterized by the minimum roughness and specimen orientation C by the maximum roughness. Apparently, surface roughness and fatigue strength as shown in Fig. 5 are reasonably correlated.

Table 2. Average surface roughness parameters vs specimen orientation.

	A	B	C
Ra [µm]	6.49	10.67	15.56
Rq [µm]	7.58	12.97	19.63
Rz [µm]	29.67	56.96	84.43

Representative fracture surfaces of A, B and C specimens are also shown in Fig. 6. Fatigue cracks initiated at the surface (top in the figure) and propagated towards the specimen interior. The fracture surface appearance indicates that the cracks started form defects just on the surface or close to it. An example is visible in Fig. 6d. The fatigue crack in the case of specimen B initiated at the defect of a pore type, which is in the figure indicated with the ellipse. The defect size is of about 200 µm. Comparison of surfaces of all three types of specimens, Fig. 6, together with the roughness measurement clearly demonstrates, that the surface quality a and subsurface defects are crucial factors determining the fatigue life of the SLM IN 718.

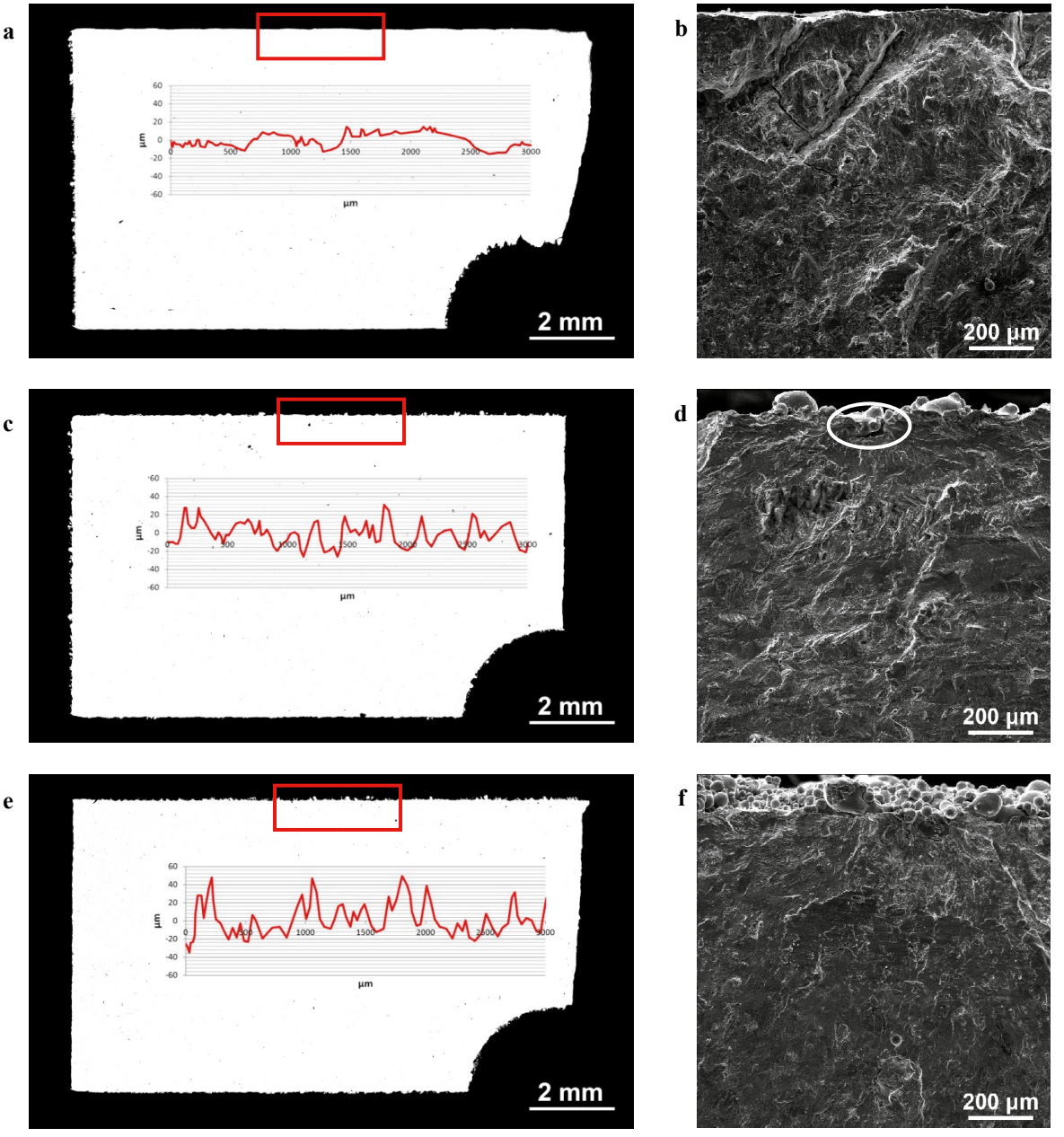

Fig. 6 As-fabricated surface roughness of SLM IN 718 specimens (a) A, (c) B, (e) C; fatigue fracture surfaces with initiation places of SLM IN 718 specimens (b) A, (d) B, (f) C.

4. Conclusions

The degree of anisotropy of the fatigue behavior of SLM IN 718 has been determined by testing specimens produced in three directions with respect to build. The directionality of the high cycle fatigue behavior demonstrated that the application of the cyclic stress in the direction of the build (as in C specimen) is the most severe for the material (i.e. shortest fatigue lives). The other two specimen orientations with respect to build (A and B specimens) show similar fatigue behaviors.

The presence of such anisotropic behavior is referred to the complex microstructure obtained by the layer-by-layer production process. The directional material response in fatigue was discussed in terms of surface roughness that was different for the three specimen directions and the fatigue crack initiation mechanisms because X-ray surface measurements revealed negligible residual stresses after the post fabrication stress relieving heat treatment.

Acknowledgements

The research was partially supported by the project Slovak VEGA grant No. 1/0685/2015. The company BEAM-IT Srl, Fornovo (PR) Italy is gratefully acknowledged for specimen production.

References

Clark, D., Bache, M.R., Whittaker, M.T., 2008. Shaped metal deposition of a nickel alloy for aero engine applications. Journal of Materials Processing Technology 203, 439-448.

Gibson, I., Rosen, D., Stucker B., 2014. Additive Manufacturing Technologies: Rapid Prototyping to Direct Digital Manufacturing. New York: Springer, pp. 498.

Knorovsky, G., Cieslak, M., Headley, T., Romig, A., Hammetter, W., 1989. Inconel 718: A Solidification Diagram. Metall. Mater. Trans. A, 20, 2149–2158.

Kruth, J. P., Levy, G., Klocke, F., Childs THC, 2007. Consolidation phenomena in laser and powder-bed based layered manufacturing, CIRP Ann-Manuf. Technol. 56, 730-759.

Konecna, R., Kunz, L., Nicoletto, G., Baca, A., 2016. Long fatigue crack growth in Inconel 718 produced by selective laser melting, International Journal of Fatigue, in press.

Nicoletto, G., Konečná, R., Kunz, L., Bača, A., 2015. Tensile and Fatigue Behavior of Ti6Al4V Produced by Selective Laser Melting, Procs. 4th International Conference of Engineering Against Failure (ICEAF IV), Skiathos, Greece.

Nicoletto G., 2016. Anisotropic high-cycle fatigue behavior of Ti-6Al-4V obtained by powder bed laser fusion, Int. J. Fatigue, under review.

VDI 3404, Additive fabrication - Rapid technologies (rapid prototyping) - Fundamentals, terms and definitions, quality parameters, supply agreements, 2014-12.

Wang, Z., Guana, K., Gaoa, M., Li, X., Chen, X., Zenga, X., 2012. The microstructure and mechanical properties of deposited-IN718 by selective laser melting. Journal of Alloys and Compounds, 513, 518-523.